

# Self-aligned fabrication process for silicon quantum computer devices

T.M. Buehler<sup>1</sup>, R.P. McKinnon<sup>1</sup>, N.E. Lumpkin<sup>1</sup>, R. Brenner<sup>1</sup>,  
 D.J. Reilly<sup>1</sup>, L.D. Macks<sup>1</sup>, A.R. Hamilton<sup>1</sup>, A.S. Dzurak<sup>2</sup> and R.G. Clark<sup>1</sup>

Centre for Quantum Computer Technology

1) School of Physics, University of New South Wales, Sydney 2052, AUSTRALIA and

2) School of Electrical Engineering, University of New South Wales, Sydney 2052, AUSTRALIA

(Dated: May 21, 2019)

We describe a fabrication process for devices with few quantum bits (qubits), which are suitable for proof-of-principle demonstrations of silicon-based quantum computation. The devices follow the Kane proposal to use the nuclear spins of  $^{31}\text{P}$  donors in  $^{28}\text{Si}$  as qubits, controlled by metal surface gates and measured using single electron transistors (SETs). The accurate registration of  $^{31}\text{P}$  donors to control gates and read-out SETs is achieved through the use of a self-aligned process which incorporates electron beam patterning, ion implantation and triple-angle shadow-mask metal evaporation.

PACS numbers: 61.72.Vv, 81.16.Nd, 85.35.-p, 85.40.Ry

Large-scale quantum computers [1] promise a massive increase in the speed of important computational tasks such as prime factorisation [2] and database searching [3]. One of the most promising schemes, which is capable of being scaled up to processors with many quantum bits (qubits), is the silicon-based solid-state quantum computer (SSQC), first proposed by Kane [4]. Such devices require the positioning of single dopant atoms to better than 10 nm: a highly challenging task. However the paradigm has a major advantage over competing proposals in that the fabrication strategy is compatible with industry-standard silicon metal-oxide-semiconductor (MOS) processing technology.

A silicon-based SSQC is depicted schematically in Figure 1. The nuclear spin (I) of single  $^{31}\text{P}$  donor atoms ( $I=1/2$ ) embedded in  $^{28}\text{Si}$  ( $I=0$ ) constitutes the qubit. 'A'-gates above the donors enable single-qubit operations by controlling the hyperfine interaction between electron and nucleus. 'J'-gates between donors enable two-qubit operations by controlling the exchange interaction between adjacent donors [4]. During the qubit read-out process, nuclear spin information is transferred to electron spin states as described by Kane [4]. Under the influence of an asymmetric gate bias, the Pauli exclusion principle dictates that electron motion between two P

donors (to form a two-electron bound state - see Fig. 1) will only take place if the electrons are in a spin-singlet state. Qubit read-out is achieved using a charge-sensitive single electron transistor (SET) to detect whether or not this charge transfer occurs, thereby allowing determination of the two-electron spin state [4]. The device must be operated at temperatures of 1 K, or below, in order to minimise qubit decoherence and to ensure that all electron spins are in their ground state.

Realization of the structure shown in Fig. 1 requires not only the ability to form ordered arrays of  $^{31}\text{P}$  atoms in  $^{28}\text{Si}$ , but also a capability to accurately align these atoms to their control gates and read-out SETs. These requirements remain relevant to variations on the original Kane design, including those utilizing either nuclear-spin qubits [5] or electron-spin qubits [? ]. Recently, it has been demonstrated [7] that P qubit arrays on Si can be fabricated using an atom-structuring approach in which a scanned probe is used to pattern a monohydride resist on a silicon surface. While this approach can be extended to produce high-precision P donor arrays on a large scale, a number of challenging steps, including subsequent epitaxial overgrowth and gate registration, have yet to be demonstrated.

This paper describes an approach to SSQC fabrication which has two key advantages over other schemes: (i) all of its steps are based upon existing semiconductor processes; and (ii) it employs a self-alignment technique for registering single donors to control gates and read-out SETs. The scheme described here is designed for few-qubit devices which will be critical for determining the feasibility of a SSQC. It is also possible to envisage modifications which would allow scale-up of the process for many-qubit array fabrication. Here we demonstrate the fabrication of an integrated array of control gates and SETs, and present a detailed strategy for self-aligning these structures to individual P atoms.

For the purposes of this paper, we consider a six-donor, four-qubit device as shown in Figure 2(a). We first outline the conceptual approach for the process,

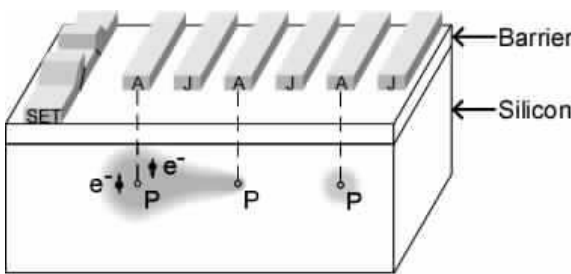


FIG. 1: Figure 1. SSQC architecture in which  $^{31}\text{P}$  atoms form an array of quantum bits in  $^{28}\text{Si}$ . The SET is used to read out the spin configuration of the two left-most donors.

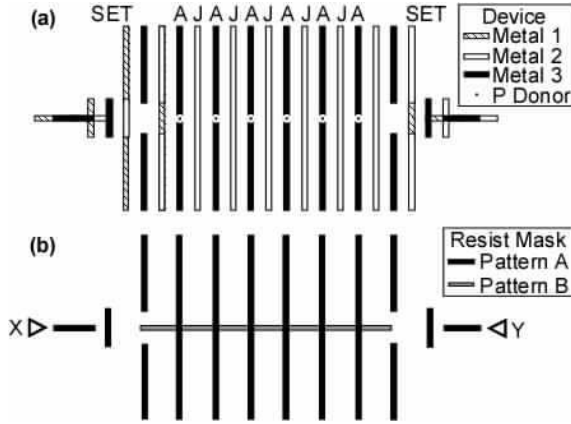


FIG. 2: Figure 2. (a) Schematic of a six-donor device. The dots represent individual P atoms. (b) The two EBL patterns required to form the structure shown in (a). The black pattern forms the gates and SETs after triple-angle shadow evaporation, while the overlap of the grey and black patterns defines the qubit locations.

then focus on a particular implementation employing poly-methylmethacrylate (PMMA), poly-methacrylic acid (PMAA) and polymethylglutarimide (PMGI) resists.

Surface metallisations for the device are defined using multi-angle shadow evaporation, which is already a well-established technique for fabricating Al/Al<sub>2</sub>O<sub>3</sub> SETs [8]. A single high-resolution electron beam lithography (EBL) step is used to create the black pattern (Pattern A) shown in Fig. 2(b). Following resist development, triple-angle shadow evaporation [9] and oxidation are performed to produce Al and Al/Al<sub>2</sub>O<sub>3</sub> structures which constitute all of the gates and SETs shown in Fig. 2(a). Although some extraneous features are produced by the shadow evaporation process, these will not significantly affect the performance of the device. The resist structure used for the shadow evaporation step (Resist A) must be able to produce a wide cavity beneath fine features in a surface layer [9] and would generally be comprised of two or more resist layers of differing sensitivity, as discussed later.

A linear array of self-aligned donors can be realized by incorporating an additional EBL step using a different resist (Resist B). The locations of the six donors in the device may be defined using the grey pattern (Pattern B) shown in Fig 2(b). The points at which Patterns A and B cross define the donor sites. Access channels for ion implantation, which extend to the substrate at these donor sites, may be opened by either wet development or dry etching. A critical requirement is that the two resist structures utilize different developer solutions or different dry etch processes.

Partial etching or development of Resist A, along with complete etching or development of Resist B produces a profile such as that shown in Figure 3(a) for ion implantation. Ions must be implanted at low energy (of

order keV) to ensure donors are located 5-20 nm below the Si/SiO<sub>2</sub> interface and with an areal dose such that on average one ion is implanted at each donor site. By Poissonian statistics, the probability that a single ion lands in each of N sites is given [?] by  $0.367^N$ . As N increases, the device yield would fall to low levels without additional strategies aimed at controlling ion placement. One such strategy involves the use of on-chip ion impact detectors which electrically register the arrival of each ion in the device, during the implant process [10]. This approach ensures that exactly N donors will be implanted in an intended N-donor device. Recent results using this technique demonstrate the detection of single <sup>31</sup>P+ ions of energy 15 keV entering an i-Si substrate [10]. This ion energy leads to an average implant depth of 20 nm, suitable for a SSQC device. In order to scale-up this process for the construction of many-qubit processors it will be necessary to localise the ion beam to a spot size smaller than the spacing between donor sites and move the beam between each site until a single ion implant event is registered. Such localisation could be achieved using a focused ion beam (FIB) or a moveable mask with a nanomachined aperture [11].

Although ion implantation is a convenient technique for introducing donors into Si, there are two aspects of the process which could impair the reliable operation of a SSQC, namely straggle of P donors from their desired locations and damage to the Si lattice. The effect of straggle has been estimated using SRIM software (Stopping and Range of Ions in Matter) and for typical donor depths of 10 nm we find a lateral straggle of order 5 nm [12]. These values suggest that it will be necessary to individually tune the gate voltages that control each donor qubit, to take into account its specific location. Lateral straggle can be improved somewhat by channelling the implant along a crystal axis, however, the amorphous SiO<sub>2</sub> barrier layer will serve to randomise the incident angle and reduce channelling.

There is limited information on damage induced by

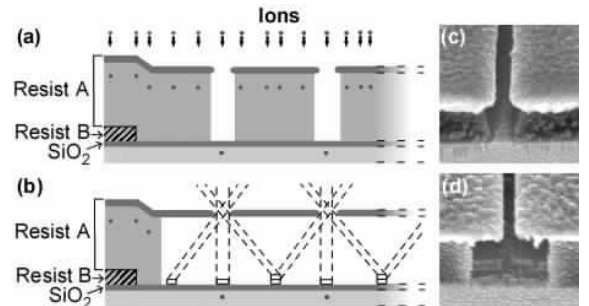


FIG. 3: Figure 3. (a) Resist profile for the ion implantation step. (b) Profile for the triple-angle evaporation process. Profiles in (a) and (b) are cross-sections along XY in Fig. 2(b). (c) SEM image of ion implantation channel in bilayer resist of PMMA (upper) and PMMA/PMAA (lower). (d) SEM image of multi-angle evaporation cavity in bilayer resist.

single implanted donors in Si, although molecular dynamics calculations [13] indicate that considerable damage may be automatically removed by self-annealing in the first picosecond after impact. Residual damage can be removed by annealing after the metallisation of the gates and removal of the resist layers. In the worst case, it may be necessary to anneal at temperatures as high as 900C in order to remove impact damage and activate the P donor electrons. Given that SET tunnel barriers are likely to be degraded above 400C during long anneal steps, it may be necessary to use a rapid thermal anneal (RTA) process for these devices. Alternatively, SETs could be fabricated in a separate EBL step after annealing [10]. Although the alignment of SETs to donors would be compromised in this case, read-out is still expected to be successful due to the demonstrated high sensitivity of SETs. An advantage of post-fabrication of the SETs is that refractory metals could be used for the gates. Some refractory metals, such as tungsten, have high melting points and also exhibit low diffusivity through SiO<sub>2</sub> barrier layers.

Following ion implantation, complete development of Resist A produces a cavity suitable for multi-angle shadow evaporation (see Fig. 3b). Any remaining Resist B on the floor of the cavity is also removed at this point. The triple-angle shadow evaporation process depicted in Fig. 3(b) produces self-aligned gate and SET structures with A-gates located directly above implanted donors, thus realizing the complete device shown in Fig. 2(a).

We now describe a particular example of the fabrication strategy outlined above which employs only wet chemical processing. Firstly, PMGI (Resist B) is prepared on a Si/SiO<sub>2</sub> substrate. Pattern B is exposed using EBL and developed with an aqueous developer. Next, a bilayer (Resist A) of PMMA and PMMA/PMAA copolymer is prepared on top of the PMGI and Pattern A is exposed. Partial development of the bilayer with an organic solvent (MIBK/IPA) is then carried out to create narrow trenches down to the PMGI. This developer solution does not affect the PMGI. Fig. 3(c) shows the profile of a partially developed bilayer cavity. Where the two EBL patterns overlap, channels extending to the substrate surface are created, through which ion implantation may be performed.

As a trial of this process, we have exposed and developed a series of lines in bilayer resist, on top of and perpendicular to a series of lines exposed and developed in PMGI (Fig. 4a). The resulting structure was etched using an HF solution and then the resist layers removed. Atomic force microscope (AFM) imaging (Figs. 4b and 4c) confirmed that etch pits in the Si/SiO<sub>2</sub> substrate were formed only where the two sets of lines overlapped.

Following ion implantation, the bilayer is fully developed and any PMGI remaining in the cavity is removed with a solvent which does not affect the bilayer. Fig. 3(d) shows the profile of a typical bilayer cavity. Triple-angle Al shadow evaporation is then performed with in-situ ox-

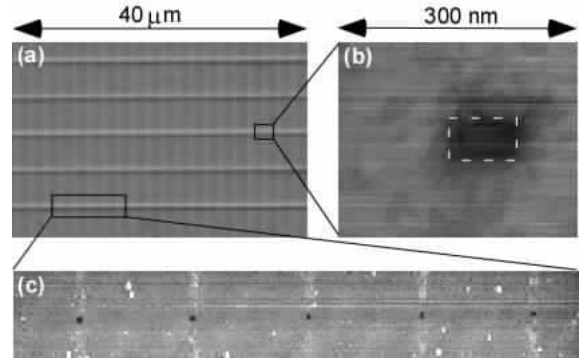


FIG. 4: Figure 4. (a) Trial cross-patterning results of EBL-defined lines in a trilayer resist, as detailed in the text. Patterning of the bottom PMGI layer is just visible as faint vertical lines. (b) and (c) AFM images of pits etched at the intersections of lines shown in (a).

idation between the first and second angle evaporation to form the Al/Al<sub>2</sub>O<sub>3</sub> tunnel junctions required for SET operation. Removal of any remaining resist then leaves the structure shown in Fig. 2(a) on the substrate surface.

The triple-angle evaporation process described above has been demonstrated using Pattern A on a bilayer resist, producing the device shown in Figure 5(a). Fig. 5(b) shows a side-view schematic of the same device indicating the various metal layers deposited during the three evaporation steps. The intended donor sites are indicated although ion implantation was not carried out on this trial device. The 50 nm-wide lines in Fig. 5(a) are the A-gates, which lie directly above the intended donor sites. The J-gates on this device are slightly wider than the A-gates due to imperfect overlaying of metal lines. The gate spacing of this device is sufficiently small to fabricate an electron-spin SSQC [?], however, it will be necessary to reduce metal linewidths to 5-10 nm to realize a nuclear-spin-based device [4?]. Such linewidths have been realized using single layer EBL resists [14] and work is underway to achieve this using our multilayer process.

We are currently integrating ion implantation into the process to produce a fully configured few-qubit SSQC device. In the first instance, a two-donor device (Fig. 6a)

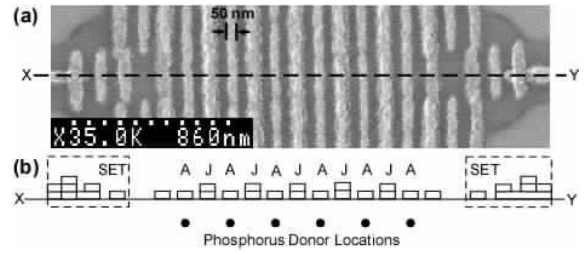


FIG. 5: Figure 5. (a) SEM image of gate and SET array for a six-donor SSQC device produced by triple-angle evaporation. (b) Cross section of the device in (a) through the line marked XY.

will be implanted. Fig. 6(b) shows the EBL patterns required to produce such a device. Fig. 6(c) is an SEM image of a demonstration metallisation of the gate and SET array formed by triple-angle shadow evaporation using Pattern A. The same device is shown on a larger scale in Fig. 6(d) revealing connections leading out to macroscopic bond pads.

Figure 7(a) shows a detailed SEM image of a typical SET fabricated by double-angle shadow evaporation on a bilayer resist. Fig. 7(b) shows the clear Coulomb blockade oscillations measured in such devices. The high transconductance ( $dG/dV_g$ ) demonstrates the sensitivity of these devices to single charge transfer events, and thus their suitability for use as qubit read-out devices in the Kane scheme. Recently, we have used two such devices in a *twin*-SET configuration to measure controlled electron transfer between two metallic dots, joined by a tunnel barrier [15].

Although here we have focused on a particular process implementation using PMGI, PMMA and PMMA/PMAA, there are a number of possible variations. To obtain the highest possible aspect ratios for the ion implantation channels, dry etching could be used in place of the wet development procedures discussed above. For example, instead of a standard bilayer structure, Resist A could be composed of a Ge layer sandwiched be-

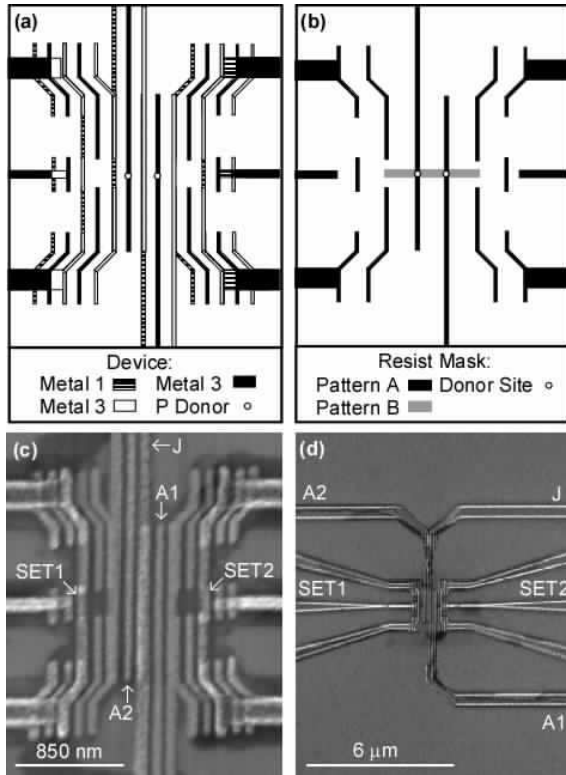


FIG. 6: Figure 6. (a) Schematic of a two-donor device. (b) The two EBL patterns required to form the structure shown in (a). (c) and (d) SEM images of the gate and SET array produced by triple-angle evaporation.

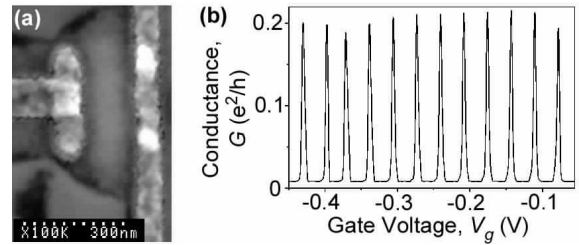


FIG. 7: Figure 7. (a) SEM image of an Al/Al<sub>2</sub>O<sub>3</sub> SET. (b) Coulomb blockade oscillations measured on a typical SET at 30 mK.

tween two organic resists [16]. Pattern A could be exposed in the top resist layer and developed, then reactive ion etching with CF<sub>4</sub> gas used to remove the exposed Ge [16]. Next, another gas could be used to anisotropically etch the underlying organic resist, thereby defining vertical-walled ion implantation channels. In another variation, the order of Resists A and B could be reversed. After ion implantation, Resist B would be removed, allowing for complete development of Resist A, followed by triple-angle shadow evaporation.

In conclusion, we have designed a process involving two EBL exposures, ion implantation and triple-angle shadow evaporation capable of producing self-aligned gate, SET and donor structures for a few-qubit SSQC. The process can utilize a variety of different resists, development and etch procedures. We have made preliminary test structures comprising gates and read-out SETs and have demonstrated that cavities for ion implantation may be formed in an organic trilayer resist structure. Work on incorporating ion implantation into our process is currently underway.

### Acknowledgement

This work was supported by the Australian Research Council, the Australian Government and by the U.S. National Security Agency (NSA), Advanced Research and Development Activity (ARDA) and the Army Research Office (ARO) under contract number DAAD19-01-1-0653.

---

[1] Steane A *Rep. Prog. Phys.* **61** 117 (1998)

[2] Shor P W *Proc. 35th Ann. Symp. on Foundations of Computer Science*, ed. S. Goldwasser (IEEE Computer Society, Los Alamitos CA) 124 (1994)

[3] Grover L K *Phys. Rev. Lett.* **79** 325 (1997)

[4] Kane B E *Nature* **393** 133 (1998)

[5] Kane B E *Fortschr. Phys.* **48** 1023 (2000); *see also* quant-ph/0003031

[6] Vrijen R, Yablonovitch E, Wang K, Jiang H W, Balandin A, Roychowdhury V, Mor T and DiVincenzo D *Phys. Rev. A* **62** 012306 (2000)

[7] O'Brien J L, Schofield S R, Simmons M Y, Clark R G, Dzurak A S, Curson N J, Kane B E, McAlpine N S, Hawley M E and Brown G W *Phys. Rev. B* **64** 161401 (2001)

[8] Fulton T A and Dolan G J *Phys. Rev. Lett.* **59** 109 (1987)

[9] Dolan G J *Appl. Phys. Lett.* **31** 337 (1977)

[10] McKinnon R P, Stanley F E, Macks L D, Mitic M, Gauja E, Peceros K, Buehler T M, Dzurak A S, Clark R G, Yang C, Jamieson D N, Prawer S, Pakes C I and McCallum J C, *to be submitted to Appl. Phys. Lett.*; Yang C, Jamieson D N, Hearne S M, Pakes C I, Prawer S D, Stanley F E, Macks L D M, Gauja E, Dzurak A S and Clark R G, *in preparation*

[11] Jamieson D N, Prawer S, Andrienko I, Brett D A, Millar V, Yang C and Cimmino A, *Proc. Int. Conf. on Experimental Implementation of Quantum Computation*, ed. R.G. Clark and A.R. Hamilton (2001)

[12] Jamieson D N (*private communication*)

[13] Marks N A, Hee Lee K and McKenzie D R *Proc. Int. Conf. on Experimental Implementation of Quantum Computation*, ed. R.G. Clark and A.R. Hamilton (2001)

[14] Chen W and Ahmed H *Appl. Phys. Lett.* **62** 1499 (1993)

[15] Buehler T B, Brenner R, Reilly D J, Hamilton A R, Dzurak A S and Clark R G, accepted for *Smart Materials and Structures* (2002)

[16] Nakamura Y, Klein D L and Tsai J S *Appl. Phys. Lett.* **68** 275 (1996)